PCCP

Accepted Manuscript

ROYAL SOCIETY OF CHEMISTRY

www.rsc.org/pccp

Journal Name

ARTICLE

From Dilute Isovalent Substitution to Alloying in CdSeTe Nanoplatelets

Received 00th January 20xx,
Accepted 00th January 20xx

DOI: 10.1039/x0xx00000x

www.rsc.org/

Ron Tenne[†a], Silvia Pedetti[†b,c], Miri Kazes*[a], Sandrine Ithurria[b], Lothar Houben[d], Brice Nadal[c], Dan Oron[a], Benoit Dubertret[b]

Cadmium chalcogenide nanoplatelet (NPL) synthesis has recently witnessed significant advance in producing more elaborate structures such as core/shell and core/crown NPLs. However, controlled doping in these structures has proved difficult because of the restrictive synthetic conditions required for the 2D anisotropic growth. Here we explore the incorporation of Tellurium (Te) within CdSe NPLs with Te concentrations ranging from doping to alloying. For Te concentrations higher than ~30%, the $CdSe_xTe_{(1-x)}$ NPLs show emission properties characteristic of an alloyed material with a bowing of the band gap for increased concentrations of Te. This behavior is in line with observations in bulk samples and can be put in the context of the transition from a pure material to an alloy. In the dilute doping regime, CdSe:Te NPLs, in comparison to CdSe NPLs, show a distinct photoluminescence (PL) red shift and prolonged emission lifetimes (LTs) associated with Te hole traps which are much deeper than in bulk samples. Furthermore, single particle spectroscopy reveals dramatic modifications in PL properties. In particular, doped NPLs exhibit photon antibunching and emission dynamics significantly modified compared to undoped or alloyed NPLs.

Introduction

Colloidal quantum wells (QWs) also termed nanoplatelets (NPLs) are a new class of quantum confined crystal architectures that has emerged in recent years as part of the prolific development in colloidal synthesis of semiconductor (SC) nanocrystals. NPLs have a well-defined thickness of only few atomic monolayers and lateral dimensions of tens of nanometers with a defect free crystallinity.[1] Whereas some of the optical and electronic properties of NPLs are reminiscent of those of 1D quantum confined systems (*i.e.* a quantum well), others, particularly those involving multicarrier interactions can be more characteristic of 3D confined systems (*i.e.* quantum dots) due to the inherently high carrier density upon optical excitation.[2]

The characteristic absorption of cadmium chalcogenide SC NPLs shows two sharp excitonic transitions from the heavy hole (HH) and the light hole (LH) valance bands to the conduction band.[3] The large surface to volume ratio and the smaller dielectric constant of the media surrounding the NPL results in a reduced excitonic radius and a large binding energy (~ 100s of meV).[4] This, in turn, gives rise to a short radiative lifetime and a small Stokes shift. Shorter radiative lifetimes can help better compete with Auger recombination whose rate is slowed due to the continuous density of states. As a result the probability for multiple photon emission by a single-particle is increased, leading to the use of NPLs in optical gain devices.[5,6] While these structures have unique optoelectronic properties, the variety of NPLs is still considerably small compared with their 3D counterparts limiting the tunability of their properties. To date, CdS, CdSe and CdTe NPLs have been synthesized, as well as heterostructures in both core/shell and core/crown geometries.[7,8] Sandwich-like core/shell structures have been shown to exhibit not only luminescence spectral tunability, but also enhanced quantum efficiency and better stability.[9,10] Type-II core/crown heterostructure NPLs such as CdSe/CdTe and CdTe/CdSe have enabled to extend NPLs emission to the near-infrared spectral region.[11-14] Yet, in both core/shell and core/crown NPLs, a few of the unique properties such as the short radiative lifetime and narrow luminescence spectrum of NPLs are somewhat compromised.[7,15] This results either from the breaking of translational symmetry or the reduction of quantum confinement. Since few-layer thick NPLs of a given material only offer discrete emission bands, a new mechanism for tuning the NPL emission while maintaining both strong confinement and translational symmetry is desired. One pathway towards the achievement of this objective is via isovalent substitution or alloying as in the $CdSe_xTe_{(1-x)}$ system, whose bulk band gap can be tuned from 1.4 eV to above 1.7 eV by composition tuning (going from x ~ 0.5 to x = 1) due to

[a] Department of Physics of Complex Systems, Weizmann Institute of Science, 76100 Rehovot, Israel
[b] ESPCI ParisTech, PSL Research University; CNRS; Sorbonne Universités, UPMC Univ. Paris 6; LPEM, 10 rue Vauquelin, F-75231 Paris Cedex 5, France
[c] Nexdot, 10 Rue Vauquelin, 75005 Paris, France
[d] Department of Chemical Research Support, Weizmann Institute of Science, 76100 Rehovot, Israel
† The first two authors contributed equally
* Corresponding author: miri.kazes@weizmann.ac.il
Electronic Supplementary Information (ESI) available: TEM, XRD, TA and PLE experimental results. Detailed analysis of the PL fit of alloyed NPLs and spectral peak asymmetry of the doped NPLs. See DOI: 10.1039/x0xx00000x

band gap bowing.[16,17] CdSeTe alloyed QDs have been successfully fabricated[18-20] and recently utilized as sensitizers in record QD sensitized solar cells exhibiting an overall efficiency of over 8%.[21,22] Working in the diluted Te-doping regime, it was shown, both experimentally and theoretically that for strongly confined structures the electron remains delocalized across the QD, while the hole is strongly localized around the Te atoms, significantly modifying the spectroscopic behavior.[23] In particular, doping results in large exciton-exciton repulsion, thus increasing the rate of Auger recombination. Another result of an increased interaction term is the elimination of the biexciton-exciton degeneracy, making the QD an effective three levels system which is desirable for many optical applications such as optical gain.[24,25] It is therefore natural to expect the CdSe:Te system to yield potential benefits also in the NPL geometry.

Here we report for the first time the synthesis and the optical properties of alloyed $CdSe_xTe_{(1-x)}$ nanoplatelets. While Te-rich NPLs are shown to exhibit spectroscopic properties similar to both pure CdSe and pure CdTe NPLs (with a modified value of the 'bulk' band gap according to the bowing parameter), the optical properties of Se-rich NPLs (x > ~ 0.7) are shown to be different, appearing to be dominated by states within the gap. Pushing this to the limit of extremely dilute Te-doping of CdSe NPLs, we use single-particle spectroscopy to show the dramatic modification of the photophysics of NPLs even by what seems to be isolated Te substitutional sites within the CdSe host.

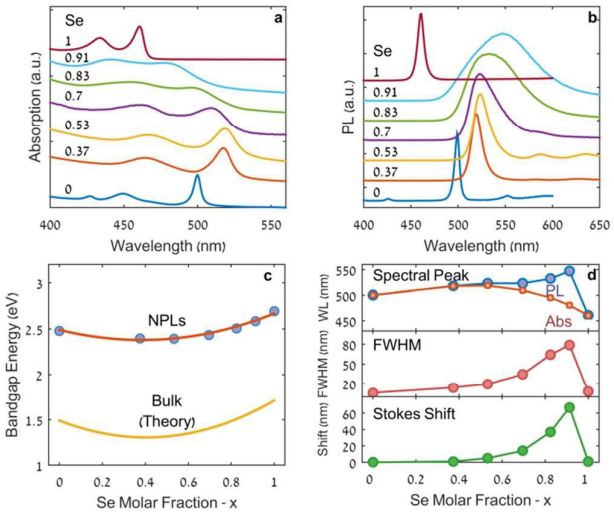

Figure 1: Optical characterization of $CdSe_xTe_{(1-x)}$ 3ML NPLs for different compositions. **a,b)** Absorption and PL spectra. **c)** Experimental band gap energy versus Se molar fraction for NPLs (circles) and theoretical curve for bulk $CdSe_xTe_{(1-x)}$ (yellow solid line). Solid red line is a fit of the experimental data with the formula given in Eq. 1 (b=0.76eV). **d)** PL peak position, Stokes shift and PL FWHM versus Se molar fraction, blue, red and green, respectivly. A schematic expected bowing dependence of the PL peak with Se composition is shown in the red line.

Results and discussion

Synthesis of three monolayers alloyed NPLs

We first synthesized 3 monolayer thick $CdSe_xTe_{(1-x)}$ nanoplatelets (3ML) while varying the two chalcogenide compositions from x = 1 to x = 0. Structurally, these NPLs have four cadmium planes in the thickness, intercalated with three anion planes. NPLs are synthesized by a modification of the well-established hot injection procedure developed by Ithurria *et al*. with TOP as the complex reagent for both Se and Te.[1] To maintain a low monomer concentration during the NPLs nucleation and growth, 1M TOPSe and TOPTe solution precursors were injected at a slow controlled rate by means of a syringe pump. The resulting Se to Te ratio in the final products was in good agreement with the nominal ratio of the precursors introduced into the reaction flask, as was corroborated by Energy Dispersive X-ray (EDX) spectroscopy (Fig. S1 in Supporting Information). Further details regarding the synthesis and characterization are provided in the Supporting Information file.

Band gap bowing in alloyed NPLs

The absorption and PL spectra of $CdSe_xTe_{(1-x)}$ alloyed NPLs of different Te to Se ratios are presented in Fig. 1a and Fig.1b ,respectively. The absorption spectra of pure CdSe and CdTe exhibit sharp excitonic peaks, characteristic of NPLs.

As the Te content decreases, *i.e.* when x increases (bottom to top in Fig. 1a), the absorption peaks gradually red-shift, and broaden slightly up to x = 0.5. For x > 0.5 we observe a blue shift accompanied by a significant broadening of the peaks. In Fig. 1c we plotted, indicatively, the edge energy values of the first excitonic peak, for the series of alloyed 3 MLs $CdSe_xTe_{(1-x)}$ NPLs as function of x measured from EDX analysis. The behavior we observe is commensurate with the known band gap bowing in bulk $CdSe_xTe_{(1-x)}$ alloys, *i.e.* parabolic trend of the energy gap with composition.[16,17]

This optical bowing may be described by the following quadratic formula:

$$(\text{Eq.1})\ E_g(x) = (1-x)E_0 + xE_1 - bx(1-x)$$

Where E0 and E1 are the band gap energies of CdTe and CdSe, and b is the bowing parameter. Fitting the experimental results with Eq.1 (Fig.1c ,red line), we extract a bowing parameter b = 0.76 eV. For comparison the band gap bowing for the bulk alloy is also shown in Fig. 1c using the calculated bowing parameter of 0.75 eV (yellow line).[17] While for spherical CdSeTe quantum dots the non-linearity of the band gap as function of the anionic composition has been already observed[20,26], it is the first time that this phenomenon is demonstrated for colloidal quantum wells.

We assume here that changes in the absorption spectra are not the result of a change in the number of monolayers in alloyed NPLs. Keeping all other experimental conditions fixed, the variation of the anionic composition is not likely to induce a significant change in thermodynamic conditions required for

nucleation of NPLs with different thicknesses. This is particularly so since for single-material NPLs, the variation of the thickness is achieved by introducing great modification to the energetic parameters of the reaction (*e.g.* temperatures or reactivity of precursors).[3] The agreement between the bowing formula (Eq. 1) and the first exciton energy trend gives further merit to this claim.

The outcome of the syntheses present a large variance in the lateral dimensions of alloyed NPLs. Its effect on the absorption line position, previously measured to a red-shift of a few nanometers, is negligible in comparison to the tens of nanometers shift observed here for alloyed NPLs.[27,28]

It is worth noting that the absorption characteristics of alloyed NPLs described here are different from those observed in spatially inhomogeneous systems such as CdSe/CdTe core/crown and core/alloyed-crown NPLs. In these, exciton transitions, characteristic of two distinct domains, are visible in the absorption spectrum: CdSe core exciton transitions and CdTe crown (or CdSeTe alloyed-crown) exciton transitions.[11-15] Both transitions' energies match those of the corresponding single-material NPLs of the same number of monolayers. On the other hand, for alloyed NPLs we observed excitonic features characteristic of single-materials NPLs, with the exception that the energies of the transitions depend on the anionic composition and shifted from pure CdTe NPLs to pure CdSe NPLs.

The maxima of the PL spectra of the alloyed 3ML thick $CdSe_xTe_{(1-x)}$ NPLs (Fig. 1d, blue symbols), red-shift continuously as x increases, even for x > 0.5. This red shift, which continues up to x = 0.9, is accompanied by an appreciable broadening of the emission peak and an increased Stokes shift (Fig. 1d, red and green symbols, respectively). Photoluminescence Excitation (PLE) measurement verifies that the PL broadening does not arise from distribution of species in the sample (Fig. S3 in the Supporting Information). Not only does the PL not follow the first excitonic absorption transition bowing behavior but there exist a seemingly abrupt transition between a 0.1 Te molar ratio concentration and a pure CdSe NPL luminescence peak wavelength. A careful multicomponent fit of the spectra, given in the Supporting Information (Fig. S4), reveals that none of the components adheres to the band gap bowing trend.

In an analogous bulk alloyed system, $ZnSe_xTe_{(1-x)}$, the observed trend of the PL shares some of the features observed here, but significantly differs in others.[29] There too, at high Te concentrations (x<0.4) PL closely follows the bowing trend. At lower Te content the Stokes shift significantly increases from less than 50meV up to a value of about 200meV (for x>0.7) due to the formation of states within the gap associated with ZnTe clusters. Notably, however, in contrast to the continuous redshift of the PL with increasing Se content observed in Fig. 1b, in bulk $ZnSe_xTe_{(1-x)}$ the PL blueshifts with increasing Te content from the bowing point to the lowest Te content measured. This comparison to $ZnSe_xTe_{(1-x)}$ bulk aids in elucidating which effects result from the properties of the bulk alloy and which are emergent due to quantum confinement. From this comparison it appears that Te-associated hole traps are much deeper (relative to the valence band edge) in quantum confined nanoplatelets than in the bulk. This is supported by a recent study of the energetics of small CdTe clusters in CdSe QDs[30], where it was shown that isolated Te substitutional sites do not act as hole traps in bulk CdSe but do lead to a deep trap (over 200mV) in 2.2nm diameter CdSe QDs.

Synthesis of Te-doped five monolayers NPLs

The stark difference between the low Te content and pure CdSe samples as well as the apparent effect of quantum confinement on the Stokes shift at the low the Te content regime are intriguing features that call for further investigation in order to better characterize the transition between alloyed and doped regimes for CdSeTe 2D nanocrystals.

We therefore set out to fabricate NPLs with low Te content and to characterize their optical properties. Importantly, for very low Te content, significant variability between the properties of NPLs within the ensemble is expected due to the stochastic nature of the number of incorporated Te atoms and the distance between them. This variance highlights the need for single-particle emission spectroscopy, as will be outlined below. Since 5ML CdSe NPLs exhibit a higher PL quantum yield, crucial for single particle measurements, it was chosen for the study on dilute Te doping.

The well-established procedure developed by Ithurria *et al*. was used for the synthesis of the 5ML NPLs.[1] Two variations on the above described synthetic procedure were therefore used to obtain sparsely doped CdSe:Te NPLs. In the first both Se and Te were introduced in an elemental powder form dispersed in ODE (termed Te-powder synthesis). In the second we used a TOPTe complex and elemental Se precursors dispersed in ODE (termed Te-TOP synthesis). Since under the temperature conditions used for this synthesis Te solubility in ODE is very limited, using the TOPTe complex while leaving the Se precursor in ODE such that only a small amount of TOP was added, allowed for increasing the amount of Te available for reaction without affecting the reaction kinetics.

Typically, these syntheses yield NPLs size of 10 nm x 25 nm as seen in the TEM images (Fig. S5 in Supporting Information). The resulting thickness was determined as 5 monolayers according to the HH and LH transitions' positions measured in the absorption spectra presented in Fig. 2a. XRD measurements, presented in Fig. S6 of the Supporting Information, match the bulk CdSe zinc blende crystal structure and show clear similarity to the CdSe NPLs XRD data published by Ithurria *et al.*[3] The presence of ~1% Te (atomic concentration) in Te-TOP synthesized NPLs is estimated from EDX studies (See Figs. S7 and S8). Although this value is within the instrument detection limit a careful comparison between EDX spectra in "on NPL" and "off NPL" position shows a clear preference for Te presence within the NPLs.

Ensemble optical spectroscopy of Te-doped NPLs

Fig. 2a presents absorption and emission spectra of Te-powder, Te-TOP and undoped CdSe nanoplatelets syntheses reaction products. Absorption spectra of the undoped and doped NPLs are almost identical. Yet, the HH transition

acquires a small red shift of 1-3 nm upon doping, commensurate with the band gap shift upon a doping level of a few percent.[16] Indeed, some control over the degree of doping by changing the Te precursor's reactivity may be suggested by this slight red-shift of the first exciton peak absorption (HH transition)

In addition, there is a red absorption tail which is shifted to higher wavelengths as measured for the Te-TOP synthesis (inset of Fig. 2a). Such a red tail in the absorption peak has been observed for Te-doped CdSe QDs and is attributed to the HOMO energy levels of the Te dopant contributing to the valance band.[23,24] Transient absorption measurements (Supporting Information Fig. S9) show a rapid transition from induced absorption to bleach within the first 1psec after the pump. This feature follows the red spectral tail seen in the linear absorption spectrum indicating a fast sub-psec cooling dynamics into long lived Te states.

While the absorption spectra strengthen the observation that the syntheses leads to NPLs formation, it only shows extremely minor modifications due to Te incorporation within the NPLs. However, major differences appear in the PL spectra of Te-doped NPLs against that of native NPLs. For the Te-powder synthesis a pronounced red tail is measured whereas for the Te-TOP synthesized NPLs a second wide peak centered around ~630nm emerges. Indeed, such sharp changes agree with the drastic difference between the CdSe and $CdSe_{0.91}Te_{0.09}$ NPLs PL spectra (Fig. 1a,b) and show that Te doping indeed strongly affects the luminescence rather than the absorption spectrum.

A variety of charge traps either by surface states or defects due to doping can generate wide spectra as the one observed in Fig. 1a by simply decreasing the band-edge emission while introducing some in-gap states which fluoresce weakly. To examine if this is indeed the case for Te-doped NPLs we measured the fluorescence quantum yield (QY) for the different syntheses' products. QY was measured to be 28% and 40% for Te-powder and Te-TOP syntheses respectively, while similar values of 16-35% were measured for several syntheses of undoped NPLs. Variations in the measured QY for undoped NPLs are probably due to differences in ligand surface passivation that occur from slight differences in the cleaning

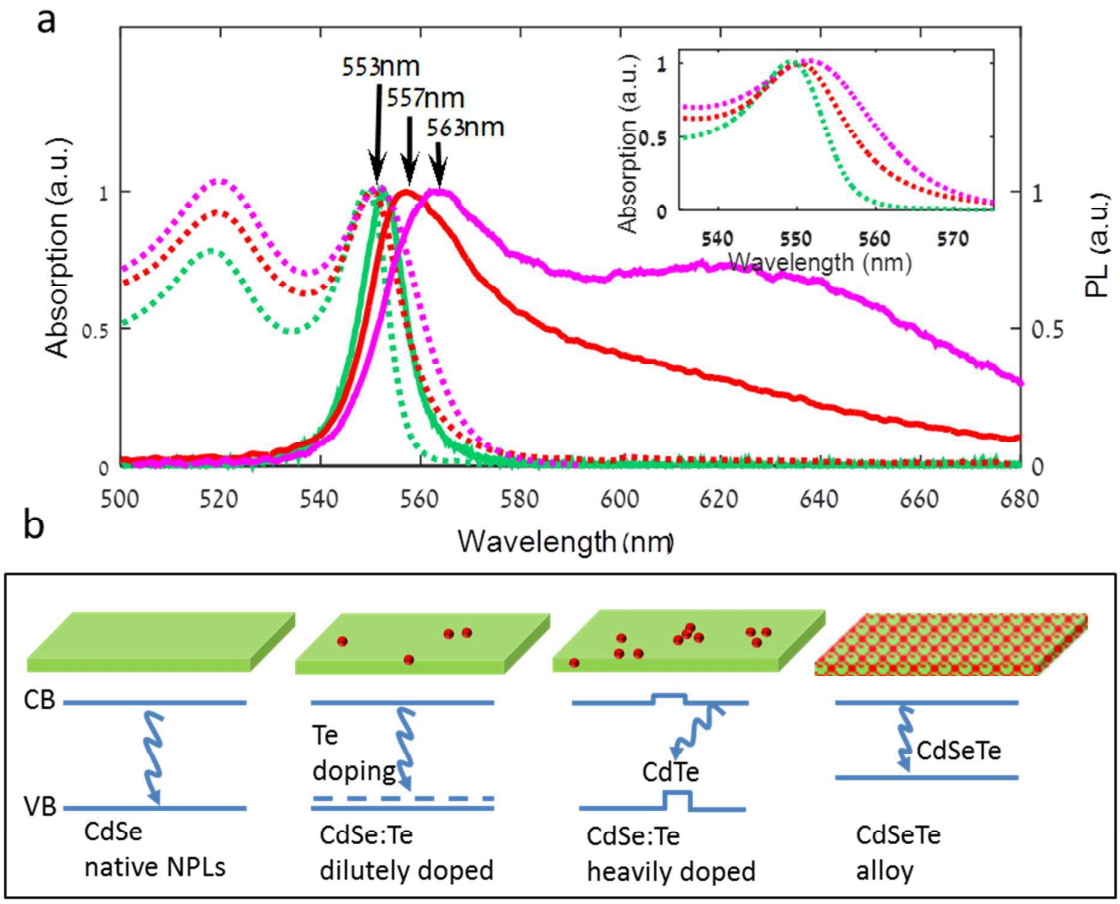

Figure 2: **a)** Absorption and photoluminescence spectra measured in ensemble, dashed and solid lines, respectively. The undoped CdSe NPLs (green), CdSe:Te NPLs by Te-powder synthesis (red), CdSe:Te NPLs by Te-TOP synthesis (magenta). **b)** A scheme of the describing the Te atoms distribution in the different NPLs syntheses products along with their energy band diagrams, from left to right: without Te dopant, with low doping density, with high doping density and an alloyed NPL.

procedure employed. The relatively high QY values for the doped NPLs (which are comparable and even slightly higher than those of undoped ones) indicate that their PL spectra broadening is not generated by surface trap emission but rather by actual substitutional doping.

Furthermore, since Te is present in the solution throughout the entire synthesizing reaction it seems likely that it is incorporated within the CdSe lattice as the NPLs grow. Segregation to the surface is unlikely due to the extremely slow expected solid state diffusion rate of Te within CdSe at the reaction temperature (240°C).[31,32] Interstitial doping of Te within the CdSe matrix seems unlikely for two reasons. First, the large ionic radius of Te_2 is larger by ~10% than that of a Se_2 ion and will therefore impose strain in any interstitial site. Additionally, such a defect would need to have an oppositely charged partner. A substantial strain field, created by the pair, close to a free standing surface causes this state to be thermodynamically unfavorable. We therefore consider the incorporation of Te in these structures, as in the alloyed NPLs, to be in substitutional sites only.

Single particle optical spectroscopy of Te-doped NPLs

It appears evident that the PL spectra of both Te incorporated NPLs syntheses are comprised of two overlapping emission peaks suggesting two different species schematically illustrated in Fig. 2b: Dilutely Te-doped NPLs (II) and NPLs with at least one CdTe cluster (*i.e.* "heavily doped") (III). The term 'CdTe cluster' refers, in this context, to two or more Te atoms occupying neighboring chalcogenide sites in the CdSe lattice.

The evidence of a multi-species synthesis product, obscuring spectroscopic features at the ensemble level, shows the importance of performing single particle spectroscopy measurements when characterizing these low doping level nanocrystals.

Single nanocrystal spectra and a time-resolved single photon correlation measured in a Hanbury-Brown and Twiss (HBT) setup were collected consecutively for each single particle. The most striking difference between doped and undoped NPLs, as revealed from all single particle measurements, is the Antibunching feature. Eq.2 defines the Antibunching factor (ABF) which quantifies to what extent a nanocrystal can be considered as a single photon emitter.

$$(\text{Eq.2})\ \text{ABF} = 100\% \cdot \frac{G^{(2)}(\tau=0) - G^{(2)}(\text{dark})}{\langle G^{(2)}(\tau>0)\rangle - G^{(2)}(\text{dark})}$$

Where, $G^{(2)}(\tau)$ is the number of photon pairs detected within a certain delay between their arrival times measured in terms of number of pulses (see insets of Fig. 3a). $G^{(2)}(\text{dark})$ refers to an estimated number of detection coincidences in which at least one detection is the result of detector dark current and $\langle G^{(2)}(\tau > 0)\rangle$ denotes an average photon pair number over pulse differences range between 3 and 30. In this scale 0% ABF is indicative of exclusively single photon emission while a 100% means no suppression of photon pair fluorescence. Typically, single QDs have been shown to exhibit a low probability of simultaneous multiple photon emission due to the rapid non-radiative Auger decay of multiply-excited states; corresponding to a value of ABF close to zero.[33-35] However, in the case of NPLs, previous works have reported a non-negligible biexciton quantum yield (BXQY) leading to appreciably larger values of ABF.[15] This feature was attributed to the extended size of the lateral dimension that results in a continuous density of states for the charges, and reduces the non-radiative Auger recombination rate. Our results for the undoped NPLs sample indeed found a distribution of ABF values for blinking, seemingly single, NPLs, ranging from about 30% to 90%. Fig. 3a shows a ABF histogram of single NPL for the undoped (green), doped Te-powder (red) and doped Te-TOP (magenta) NPLs samples. One can see that while for undoped NPLs the ABF is higher than 30% and reaches values as high as 90 %, for both doped syntheses ABF doesn't exceed 10 % for the majority of NPLs. This result matches intuition gained by previous research on Te-doped QDs, in which it was indirectly inferred that the biexciton Auger lifetime was reduced by the incorporation of a Te dopant.[36,37] This reduction was explained to stem from the Te dopant acting as a deep hole-trap, increasing the local hole-hole Coulomb interaction and therefore increasing the rates of Auger recombination.[30,37] In a similar manner Tessier *et al*. have shown that for CdSe/CdS core/crown NPLs[15], decreasing the CdSe core size yielded a lower ABF in single particle emission. Similarly to the mechanism suggested here, the increased probability for Auger recombination was explained by the strong confinement of holes within the small CdSe cores.

While this ABF measurement clearly shows a drastic effect of Te incorporation within CdSe NPLs that cannot be revealed in an ensemble measurement, it doesn't address the question of inhomogeneity within the doped synthesis products, as ABF has a continuous distribution for Te-incorporated NPLs. We have therefore measured, alongside the HBT measurements, the PL spectrum for each of the single NPLs analyzed. Three typical single NPL emission spectra are given in the insets of Fig. 3b and 3c. While the single undoped NPLs' spectra (green) resemble their ensemble spectra (Fig. 2a), featuring a narrow peak centered at ~555nm, the Te-incorporated samples display two distinct types of spectra: a ~560nm peaked spectrum with an asymmetric red tail (blue) and a second type with a symmetric wide peak centered at ~650nm (orange). To analyze the difference between those two types of spectra Fig. 3b and 3c present a scatter plot of single NPLs' spectral peak *versus* peak asymmetry for the Te-powder and Te-TOP samples respectively (see Supporting Information for definition of peak asymmetry). Native NPLs (Fig. 3b and 3c green circles), shown for comparison, exhibit symmetric spectra peaking at 555nm, whereas for both Te-incorporating syntheses two groups of NPLs species are evident (Fig. 3b and 3c blue and orange circles). The first group has highly asymmetric spectra with peak centered at 555-560nm whereas the second displays symmetric spectra with peak emission widely distributed between 600-700nm.

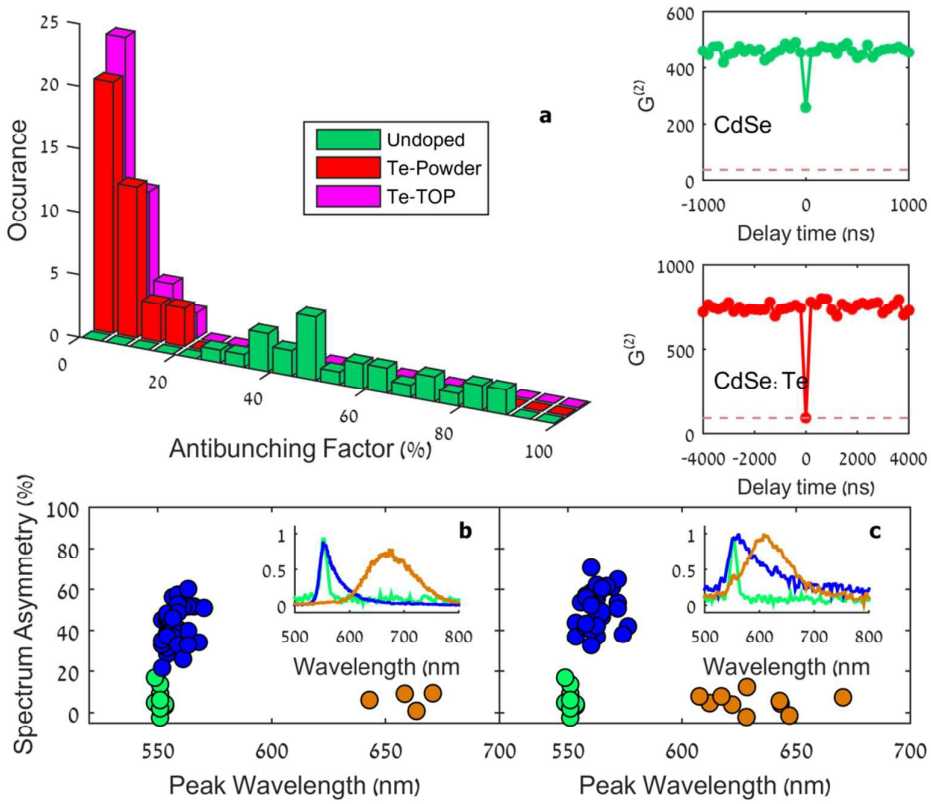

Figure 3: Distinguishing synthesis outcome through single particle spectroscopy. **a)** Histogram of the Antibunching factor for the undoped synthesis (green), doped synthesis Te-powder (red) and Te-TOP synthesis (magenta). Insets present two representative $G^{(2)}$ curves for an undoped (top) and a doped (bottom) NPL. Dashed lines in the insets represent the $G^{(2)}$ dark level used in Eq.2 . **b,c)** Scatter plot of single NPL's spectrum peak wavelength and peak asymmetry for the Te-powder doped synthesis (b) and Te-TOP doped synthesis (c). In both figures the lightly doped NPLs (blue) and heavily doped NPLs (orange) are plotted together with the undoped (native) synthesis NPLs (green) for comparison. The asymmetry is defined as the difference between the area under the red side and the blue side of the PL peak divided by the total area of the PL. Representative spectra of individual NPLs are given in the inset of each figure following the same color code as (b) and (c).

The first species, displaying heavy tailed spectra, resembles results obtained for Te-doped CdSe QDs shown to include only a single Te emitting center, in which the PL emission was shifted to the red and developed a red tail.[23,30] While the red tail line shape is similar to QDs, the red shift of the peak is much more pronounced in 3D nanocrystals compared to the ~5 nm shift measured here for NPLs.[32]

While isolated dopant atoms (Fig. 2b, second diagram) may explain the spectra of the first species, the second, with a broadened symmetric red shifted emission, can be attributed to NPLs with at least one CdTe cluster (Fig. 2b, third diagram). Such a cluster leads to a distribution of trap states. Indeed similar single particle spectra were observed in Te-doped QDs.[23] In addition, it was shown that for core/crown CdTe/CdSe NPLs with small cores the absorption is dominated by the large CdSe crown while the emission is dominated by the low energy type-II spatially indirect exciton.[11,13]

The main difference, with respect to this analysis, between the two syntheses' products is the higher occurrence of the red peaked species in the doped Te-TOP sample, suggesting that these are indeed products of higher Te concentration NPLs, which result in the formation of CdTe clusters.

Notably, PLE measurements at all emission wavelengths, match the linear absorption spectra of NPLs (see for example Supporting Information Fig. S10), indicating that the absorption originates from the "bulk" of the CdSe matrix while the emission originates from the Te states. In addition, this serves as direct proof that indeed all observed emissions are due to the excitation of doped NPLs and not other species such as CdTe or alloyed NPLs.

Photoluminescence transients in alloyed and doped NPLs

To further elucidate the transition from doped to alloyed NPLs we explore the differences in the temporal transients of luminescence. While for the alloyed samples ensemble (in solution) measurements are sufficient to extract the dynamics, in the case of Te-doped NPLs the reaction products are mixtures of two species and therefore have to be studied as

single particles. In order to compare the outcome of ensemble and single particle measurements we average the transients of over ~30 NPLs of the lightly doped species and ~10 NPLs of the heavily doped species. To overcome the issue of excessive blinking of NPLs (like QDs) on a substrate we post-select detections that were measured only during the 'on' state emission by using a threshold (see Supporting Information).

In both native CdTe (black) and CdSe (green) NPLs' PL transient, shown in Fig. 4, the most prominent component is a fast one with lifetime of ~1ns and ~2ns respectively. As the concentration level decreases below 30% Te, a long lifetime component (~50 ns) becomes more dominant. Finally, for the 9 % Te sample, the lifetime curve is composed entirely of a single exponent. At this point the trend of lifetime increase

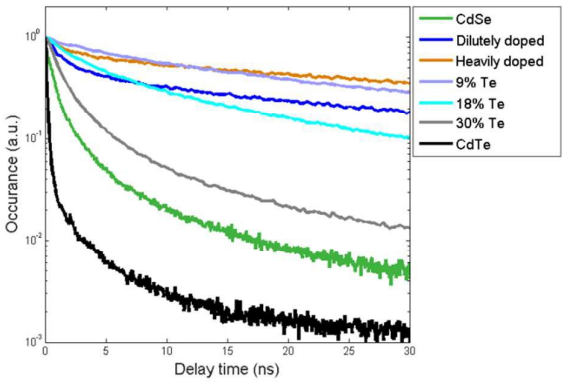

Figure 4: PL transients of pure CdSe (green) and CdTe (black) NPLs are shown together with similar curves measured for alloyed NPLs of different Te compositions (9% Te purple, 18% Te cyan and 30% Te grey). Lifetime curves of the dilutely doped and heavily doped NPLs, derived from averaging of single particle luminescence are shown in blue and orange, respectively.

inverts and for heavily Te-doped species the fast lifetime component re-appears, becoming even more visible in the case of lightly doped NPLs.

A similar trend of an emergent long lifetime component was shown in Te-doped CdSe QDs going from pure CdSe QDs to 5% Te content nanoparticles.[23] Furthermore, a full systematic lifetime study measured for the bulk $ZnSe_xTe_{(1-x)}$ system shows initially an increase of average lifetime with increased Te concentration up to 10% followed by a return to an emission lifetime characteristic of pure ZnSe for higher Te concentrations.[38] In addition, the stretched exponential behavior of the lifetimes in this system was explained by the hopping-transport model where the transfer of excitons from shallow to deep Te localized states provide multi decay paths.[39] Such multi-exponential transients are more difficult to analyze in this system since pure CdSe and CdTe NPLs themselves present multiple time scales in the PL transients. However, qualitatively, we can see in Fig. 4 that higher Te concentration curves (e.g. 18% and 30%) appear "smoother", that is they cannot be fit by just one or two exponentials but hint at a distribution of recombination rates as the model described in reference 39 predicts.

For the $ZnSe_xTe_{(1-x)}$ bulk system in the low Te concentration side, as the Te content increases the hybridization with valence band edge states results in the decrease of the PL lifetime and linewidth. In contrast, in the low Se content regime, there is no change since Se levels lie above the top of the valance band in ZnTe.[40]

Conclusions

In conclusion, we have shown the complete optical transition from lightly Te-doped CdSe NPLs to $CdSe_xTe_{1-x}$ NPLs alloys. We have demonstrated the synthesis of Te-doped CdSe NPLs and an extensive control over the synthesis of alloyed NPLs. For Te concentration higher than ~30%, the $CdSe_xTe_{(1-x)}$ NPLs show a bowing phenomenon of the band gap for increased concentration of dopant analogous to an alloyed bulk material. However, the PL peak wavelength doesn't follow the same trend at lower Te concentration and instead redshifts with decreasing Te content, creating a sharp transition from pure CdSe NPLs. This is due to the presence of Te substitutional sites which act as deep hole traps and dominate the luminescence spectrum. Reducing the Te concentration towards the dilute doping regime reveals a stepwise drastic change in the PL spectra, which we associate with a transition from small CdTe clusters to isolated Te substitutional sites. Furthermore, lifetime measurements show a dramatic increase from the pure CdSe NPLs case to the doped ones associated with a Te deep hole trap. For increased Te content (above ~10%) the lifetime gradually decreases back to values similar to the single material nanoplates, indicating the absence of trap states within the gap. The stark difference between pure and doped NPLs is also shown in photon antibunching measurements, where the probability of emitting photon pairs is highly reduced in doped NPLs. These findings manifest the stepwise transition from pure CdSe NPLs to Te-doped NPLs and then a continuous gradual transition for $CdSe_xTe_{(1-x)}$ alloyed NPLs of increased Te content.

Materials and methods

Alloyed NPLs synthesis.

A three-neck flask was charged with 120 mg of $Cd(Myr)_2$ (0.21 mmol) in 12 mL of ODE. The mixture was degassed under vacuum at RT for 30 min. Then, under Ar flux, the temperature was increased to 240 °C and 60 mg of $Cd(OAc)_2 \bullet 2H_2O$ (0.23 mmol) and 160 mg of $Cd(prop)_2$ (0.62 mmol) were added. After 1 min, a solution composed of 150 µL of a variable ratio of TOPTe 1 M and TOPSe 1 M, and 200 µL of OA (0.63 mmol) in 2 mL of ODE were added using a syringe pump. The injection rate was fixed at 8 mL/h. After 30 min from the onset of the injection, the heating mantle was removed and the mixture cooled down. At 100 °C, 1 mL of OA was added. At room temperature, 15 mL of hexane and 10 mL of EtOH were added to the mixture. NPLs were precipitated by centrifugation at

5000 rpm for 5 min and the selective precipitation was repeated 2 times replacing hexane with toluene. Finally, NPLs precipitated were re-dissolved in 5 mL of toluene.

To synthesize alloyed $CdSe_xTe_{(1-x)}$ NPLs with variable composition, we performed several experiments were the nominal molar ratio Se:Te varied between 100:0, 90:10, 80:20, 66.6:33.4, 50:50, 33.4:66.6 and 0:100.

Doped NPLs synthesis.

A mixture of 0.3 mmol cadmium myristate ($Cd(Myr)_2$) and 15mL of octadecene (ODE) are put in a flask and degassed under vacuum at 100 oC for 1 hour. The temperature is then raised to 240 oC under argon flow. A mixture of Selenium (Se) and Tellurium (Te) consisting of 0.075 mmol of Se and 0.075 mmol of Te dispersed in 1mL of ODE is rapidly injected at 240°C. Alternatively, a Se/Te stock consisting of 0.135 mmol Se dispersed in 1 mL ODE mixed with 0.1 mL of TOPTe stock (0.15 mmol Te and 0.15 mmol trioctylphosphine (TOP) dissolved in 1mL ODE under moderate heat until a clear greenish solution is obtained) is used. After 20 sec 0.3 mmol of cadmium acetate ($Cd(OAc)_2$•1H2O) is dispensed into the flask. The synthesis is monitored by absorption and photoluminescence measurements using a UV-VIS spectrophotometer (V-670, JASCO) and a fluorimeter (USB4000, Ocean Optics). After ~10min 4mL of oleic acid (OA) is injected into the flask and the growth is quenched by lowering the temperature. The NPLs were then precipitated out from chloroform and redispersed in hexane.

Single particle spectroscopy.

Highly dilute solutions ($\sim 10^{-12} M$ NPLs' concentration) of doped and pure 4ML NPLs in Hexane were spin coated onto a glass cover slip. The sample was measured in an optical setup built around a commercial microscope (Axiovert 200, Zeiss). 473nm 100ps laser pulses at 5-20MHz repetition rate (EPL 470, Edinbrough Instruments) were tightly focused through a 1.3 N.A. objective lens (Zeiss) to a diffraction limited spot. PL light was collected through the same objective passing through a dichroic mirror (488LP Semrock) and a long-pass dielectric filter (488LP Semrock). Light was then steered into one of two ports. The first is a Hanbury-Brown and Twiss setup in which light, including the entire PL spectrum, is coupled into a split-fiber coupled to two Avalanche Photo Diodes (APDs) (Perkin Elmer SPCM). The APDs' signal is routed into a timing module (Picoquant, Hydraharp 400) and is analyzed digitally with MATLAB software. The second port is a fiber coupled spectrometer (Princeton Instruments, Acton SP2300i) equipped with a 300gr/mm grating whose output is measured with a cooled CCD (Pixis, Princeton Instruments).

Approximately 100 single particles of the undoped, doped Te-powder and Te-TOP samples were examined altogether.

Acknowledgements

The authors wish to thank Dr. Iddo Pinkas for the transient absorption measurements.

Notes and references

1 S. Ithurria, B. Dubertret, *J. Am. Chem. Soc.,* 2008, **130**, 16504-16505.
2 S. Ithurria, G. Bousquet, B. Dubertret, *J. Am. Chem. Soc.,* 2011,**133**, 3070–3077.
3 S. Ithurria, M. D. Tessier, B. Mahler, R. P. S. M. Lobo, B. Dubertret, A. L. Efros, *Nat. Mater.,* 2011, **10**, 936–941.
4 R. Benchamekh, N. A. Gippius, J. Even, M. O. Nestoklon, J. M. Jancu, S. Ithurria, B. Dubertret, A. L. Efros, P. Voisin, *Phys. Rev. B,* 2014, **89**, 035307.
5 J. Q. Grim, S. Christodoulou, F. Di Stasio, R. Krahne, R. Cingolani, L. Manna, I. Moreels, *Nat. Mater.,* 2014 **9**, 891–895.
6 C. She, I. Fedin, D. S. Dolzhnikov, A. Demortiere, R.D. Schaller, M. Pelton, D.V. Talapin, *Nano Lett.,* 2014, **14**, 2772-2777.
7 M. D. Tessier, B. Mahler, B. Nadal, H. Heuclin, S. Pedetti, B. Dubertret, *Nano Lett.,* 2013, **13**, 3321-3328.
8 A. Prudnikau, A. Chuvilin, M. Artemyev, *J. Am. Chem. Soc.,* 2013, **135**, 14476-14479.
9 B. Mahler, B. Nadal, C. Bouet, G. Patriarche, B. Dubertret, *J. Am. Chem. Soc.,* 2012, **134**, 18591-18598.
10 S. Ithurria, V. Talapin, *J. Am. Chem. Soc.,* 2012, **134**, 18585-18590
11 S. Pedetti, S. Ithurria, H. Heuclin, G. Patriarche, B. Dubertret, *J. Am. Chem. Soc.,* 2014, **136**, 16430-16438.
12 K. Wu, Q. Li, Y. Jia, J. R. McBride, Z. Xie, T. Lian, *ACS Nano* 2015, **9**, 961-968.
13 A. V. Antanovich, A. V. Prudnikau, D. Melnikau, Y. P. Rakovich, A. Chuvilin, U. Woggon, A. W. Achtsteine, M. V. Artemyev, *Nanoscale,* 2015, **7**, 8084-8092.
14 Y. Kelestemur, M. Olutas, S. Delikanli, B. Guzelturk, M. Z. Akgul, H. V. Demir, *J. Phys. Chem. C,* 2015, **119**, 2177.
15 M. D. Tessier, P. Spinicelli, D. Dupont, G. Patriarche, S. Ithurria, B. Dubertret, *Nano Lett.,* 2014, **14**, 207–213.
16 H. Tai, S. Nakashima, S. Hori, *Phys. Status Solidi A,* 1975, **30**, K115.
17 S. Wei, S. B S. B. Zhang, A. Zunger, *Journal of Applied Physics*, 2000, **87**, 1304-1311.
18 R. E. Bailey, S. Nie, J. Am. Chem. Soc. 2003, **125**, 7100-7106.
19 G. Liang, L. i, H. Liu, J. Zhang, C. Burda, J. Zhu, *Chem. Commun. (Cambridge, U. K.),* 2010, **46**, 2974-2976,
20 L. Liao, H. Zhang, X. Zhong, *J. Lumin.,* 2011, **131**, 322.
21 K. Zhao, Z. Pan, I. Mora-Sero, E. Canovas, H. Wang, Y. Song, X. Gong, J. Wang, M. Bonn, J. Bisquert, X. Zhong, *J. Am. Chem. Soc.,* 2015, **137** (16), 5602-5609
22 Z. Pan, K. Zhao, J. Wang, H. Zhang, Y, Feng, X. Zhong, *ACS Nano,* 2012, **7**, 5215–5222.
23 T. Franzl, J. Muller, T. A. Klar, A. L. Rogach, J. Feldmann, D. V. Talapin, H. , J. Weller, *J. Phys. Chem. C,* 2007, **111**, 2974–2979.
24 A. Avidan, D. Oron, Nano Lett. 2008, **8**, 2384-2387.
25 O. Lahad, N. Meir, I. Pinkas, D. Oron, *ACS Nano,* 2015, **9**, 817-824.
26 R. E. Bailey, S. Nie, *J. Am. Chem. Soc.* 2003, **125**, 7100
27 C. Bouet, M. D.Tessier, S. Ithurria, B. Mahler, B. Nadal, B. Dubertret, *Chem. Mater.*, 2013, **25**, 639–645
28 S. Pedetti, B. Nadal, E. Lhuillier, B. Mahler, C. Bouet, B. Abécassis, X. Xiangzhen, B. Dubertret, *Chem. Mater.*, 2013, **25**, 2455–2462
29 M. J. Brasil, R. E. S. P. Nahory, F. S. Turco-Sandroff, H. L. Gilchrist, R. J. Martin, *Appl. Phys. Lett.,* 1991, **58**, 2509.
30 L. Zhang, Z. Lin, J.W. Luo, A. Franceschetti, *ACS Nano,* 2012, **6**, 8325-8334.
31 V. Leute, H. M. Schmidtke, W. Stratmann, A. Kalb, *Berichte der Bunsengesellschaft fur physikalische Chemie,* 1983, **87.6**, 483-490

32 B. Koo, B. A. Korgel, Nano Lett. 2008, **8**, 2490-2496.
33 P. Michler, A, Imamoglu, M.D. Mason, .J. Carson, G.F. Strouse, S.K. Buratto, *Nature,* 2000, **406**, 968-970.
34 B. Lounis, H.A. Bechtela, D. Gerionc, P. Alivisatos, W.E. Moernera, *Chem. Phys. Lett.,* 2000, **329**, 399–404.
35 X, Wang, X. Ren, K. Kahen, M.A. Hahn, M. Rajeswaran, S. Maccagnano-Zacher, J, Silcox, G.E. Cragg, A.L. Efros, T.D. Krauss, *Nature,* 2009, **459**, 686-689.
36 A. Avidan, Z. Deutsch, D. Oron, *Phys. Rev. B: Condens. Matter Mater. Phys.,* 2010, **82**, 165332.
37 A. Avidan, I. Pinkas, D. Oron, *ACS Nano*, 2012, **6**, 3063-3069.
38 Y.C. Lin, W.C. Chou, C. Fan, T. Ku, F.K. Ke, W.J. Wang, S.L. Yang, W.K. Chen, W.H. Chang, C.H. Chia, *Appl. Phys Lett.,* 2008, **93**, 241909.
39 B. Sturman, E. Podivilov, M. Gorkunov. M., *Phys. Rev. Lett.,* 2003, **91**, 176602.
40 J. Wu, W. Walukiewicz, K.M. Yu, J.W. Ager, E.E. Haller, I. Miotkowski, A.K. Ramdas, CH. Su, I.K. Sou, R.C.C. Perera, J.D. Denlinger, *Phys. Rev. B: Condens. Matter Mater. Phys,* 2003, **67**, 035207.